JOC Article

Penetration of Negatively Charged Lipid Interfaces by the Doubly Deprotonated Dipicolinate†

Debbie C. Crans,*,‡ Alejandro M. Trujillo,‡ Sandra Bonetti,‡,§ Christopher D. Rithner,‡ Bharat Baruah,‡ and Nancy E. Levinger‡

Department of Chemistry, Colorado State University, Fort Collins, Colorado 80513, and Department of Chemistry, Colorado State University—Pueblo, Pueblo, Colorado 81001-4901

crans@lamar.colostate.edu

Received July 31, 2008

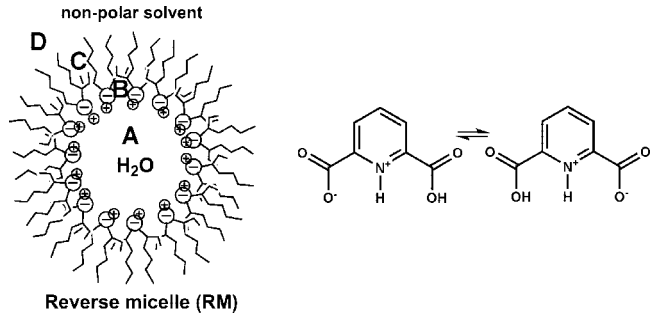

The possibility that a negatively charged organic molecule penetrates the lipid interface in a reverse micellar system is examined using UV−vis absorption and NMR spectroscopy. The hypothesis that deprotonated forms of dipicolinic acid, H_2dipic, such as Hdipic$^-$ and dipic^{2-}, can penetrate the lipid interface in a microemulsion is based on our previous finding that the insulin-enhancing anionic [VO_2dipic]$^-$ complex was found to reside in the hydrophobic layer of the reverse micelle (Crans et al. *J. Am. Chem. Soc.* **2006**, *128*, 4437−4445). Penetration of a polar and charged compound, namely Hdipic$^-$ or dipic^{2-}, into a hydrophobic environment is perhaps unexpected given the established rules regarding the fundamental properties of compound solubility. As such, this work has broad implications in organic chemistry and other disciplines of science. These studies required a comprehensive investigation of the different dipic species and their association in aqueous solutions at varying pH values. Combining the aqueous studies using absorption and NMR spectroscopy with those in microemulsions defines the differences observed in the heterogeneous environment. Despite the expected repulsion between the surfactant head groups and the dianionic probe molecule, these studies demonstrate that dipic resides deep in the hydrophobic portion of the reverse micellar interface. In summary, these results provide evidence that ionic molecules can reside in nonpolar locations in microheterogeneous environments. This suggests that additional factors such as solvation are important to molecule location. Documented ability to penetrate lipid surfaces of similar charge provides a rationale for why specific drugs with less than optimal hydrophobicity are successful even though they violate Lipinski's rules.

Introduction

The nature of organic compounds defines their properties and reactions. For example, the rules of solubility, ergo that "like-dissolves-like", are taught to beginning chemistry students to explain why reactions such as those involving 2-oxazolines[1] take place in organic solvents. Solvents dictate how molecules react[1−4] and can be used to establish a chiral environment[5] such as exemplified in the work by the late Albert I. Meyers detailing

* To whom correspondence should be addressed. Phone: 970-491-7635.
‡ Colorado State University, Fort Collins.
§ Colorado State University—Pueblo.
† This work is dedicated to Albert I. Meyers. You are missed. Your love for life and chemistry was contagious and lives on within us.

(1) Gant, T. G.; Meyer, A. I. *Tetrahedron* **1994**, *50*, 2297–2360.
(2) Meyers, A. I.; Rieker, W. F.; Fuentes, L. M. *J. Am. Chem. Soc.* **1983**, *105*, 2082–2083.
(3) Shimano, M.; Meyers, A. I. *J. Org. Chem.* **1995**, *60*, 7445–7455.
(4) Lemieux, R. M.; Meyers, A. I. *J. Am. Chem. Soc.* **1998**, *22*, 5453–5457.
(5) Elworthy, T. R.; Meyers, A. I. *Tetrahedron* **1992**, *48*, 2589–2612.

10.1021/jo801707y CCC: $40.75 © 2008 American Chemical Society
Published on Web 11/18/2008

SCHEME 1. Four Structures of H_2dipic in Different Protonation States Are Shown along with Their Respective Equilibria with pK_a Values[16]

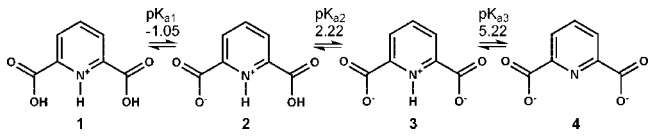

approaches in enantiomeric synthesis. Solubility is also a critical consideration in the design of compounds targeted for use in alleviation of diseases. Ideally, potential drugs adhere to the few rules defined by Lipinski which state that cell penetration is optimal when compounds possess a low molecular weight, a small number of H-bonds as both an acceptor and donor, a reasonable partition coefficient in hydrophobic solvents, and overall neutral charge.[6] Many drugs currently on the market are known to violate these simple rules and, regardless of these tenets, penetrate membranes and enter cells with relative ease. We became interested in penetration of lipid interfaces because one of the vanadium compounds that we had demonstrated to be an effective antidiabetic agent, the negatively charged oxovanadium dipicolinate $[VO_2dipic]^-$, is found to reside deep into the interface of microemulsions.[7] Since related systems are currently in phase II clinical trials,[8,9] fundamental information regarding related systems is important. In this work, we investigate the solubility of an aromatic carboxylic acid, dipicolinic acid (dipic). These studies relate to how the ligand of the $[VO_2dipic]^-$ complex interacts with lipid interfaces, and we will specifically investigate whether the dipic ligand, a doubly charged dianion at pH 7, can penetrate model lipid interfaces as recently suggested in the controversy regarding the ability of aromatic acids to partition in hydrophobic environments.[10−12] To test this hypothesis, the behavior of this ligand in aqueous solution is contrasted to its properties in the heterogeneous environment of the reverse micelles.

H_2dipic is a polar aromatic acid that in the acidic form is soluble in organic and chlorinated solvents and thus can penetrate lipid interfaces[10−14] and be solubilized in hydrophobic environments.[15] In the mono- and dianionic form, the dipic is soluble in aqueous solution at a pH above the two pK_a values 2.22 and 5.22, as shown in Scheme 1.[16] Depending on the pH, dipic assumes various forms. From left to right, we show the cationic dipic ligand, found only in highly acidic conditions at or below pK_a −1.05,[16] the neutral H_2dipic ligand that prevails near pH 4, then the monoprotonated form prevalent at pH 5.5, and finally, the fully deprotonated form at pH 7 and above. These forms and their properties are likely key to the transport of this and other simple acids and fatty acids that are known to cross cell membranes.

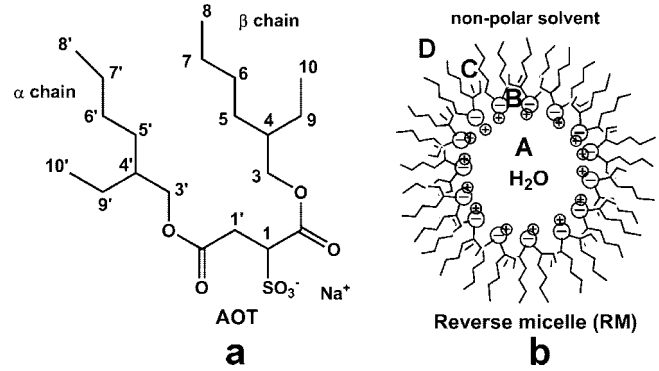

FIGURE 1. Illustrated structure of AOT (a) and an idealized reverse micelle (b) with labeled locations (A, B, C, and D) included. Labels are as follows: water pool interior (A), aqueous interface (B), surfactant tails (C), and the nonpolar solvent exterior (D).

A range of methods has been employed to examine the structure of dipic in aqueous solutions.[16−20] UV−vis studies suggested that dipicolinates associate very strongly in aqueous solution from pH 3 to 5.[16,17] Both dimeric and polymeric forms are likely to exist, although there is some disagreement in the literature on which form predominates under specific conditions.[16−20] Associative processes of dipic[16,17,21−23] are favorable when fewer water molecules are present, contribute to the penetration of the dipic molecule in lipid interfaces, and can be observed by UV−vis spectroscopy.[16−18,23−27]

Biphasic systems and microemulsions are heterogeneous systems used to solubilize compounds and facilitate reactions that would not easily take place in conventional homogeneous systems.[28] In microemulsions, multiple regimes exist with different polarities, and details of the interactions of the lipid layer constituents with water and the organic solvent can be investigated.[24] A common surfactant sodium bis(2-ethylhexyl)sulfosuccinate, abbreviated AOT, Figure 1, organizes into reverse micelles, that is, isolated aqueous droplets delineated from a continuous organic phase by a lipid interface. The reverse micelles illustrated in Figure 1b are described by a $w_0 = [H_2O]/[AOT]$ that is proportional to their size.[29−31] The simplicity of these structures and their convenient preparation[30,32] makes them a desirable system for experimentation.

In this paper, we investigate the interactions between dipic ligand and AOT microemulsions. In this work, we characterize

(6) Lipinski, C. A.; Lombardo, F.; Dominy, B. W.; Feeney, P. J. *Adv. Drug Del. Rev.* **1997**, *23*, 3–25.
(7) Crans, D. C.; Rithner, C. D.; Baruah, B.; Gourley, B. L.; Levinger, N. E. *J. Am. Chem. Soc.* **2006**, *128*, 4437–4445.
(8) Willsky, G. R.; Goldfine, A. B.; Kostyniak, P. J.; McNeil, J. H.; Yang, L. Q.; Khan, H. R.; Crans, D. C. *J. Inorg. Biochem.* **2001**, *85*, 33–42.
(9) McNeil, J. H.; Yuen, V. G.; Hoveyda, H. R.; Orvig, C. *J. Med. Chem.* **1992**, *35*, 1489–1491.
(10) Grime, J. M. A.; Edwards, M. A.; Rudd, N.; Umwin, P. R. *Proc. Nat. Acad. Sci. U.S.A.* **2008**, *105*, 14277–14282.
(11) Saparov, S. M.; Antonenko, Y. N.; Pohl, P. *Biophys. J.* **2006**, *90*, L86–L88.
(12) Thomae, A. V.; Wunderli-Allenspach, H.; Kramer, S. D. *Biophys. J.* **2005**, *89*, 1802–1811.
(13) Overton, C. E. *Vierteljahsschr. Naturforsch. Ges. Zuerich* **1899**, *44*, 88–135.
(14) Al-Awqati, Q. *Nat. Cell Biol.* **1999**, *1*, E201–E202.
(15) Dupont-Leclercq, L.; Giroux, S.; Henry, B.; Rubini, P. *Langmuir* **2007**, *23*, 10463–10470.
(16) Peral, F.; Gallego, E. *Spectrochim. Acta Part A* **2000**, *56*, 2149–2155.
(17) Peral, F. *J. Mol. Struct.* **1992**, *266*, 373–378.
(18) Wasylina, L.; Kucharska, E.; Weglinski, Z.; Puszko, A. *Khim. Geterotsiklich. Soedin.* **1999**, 210–218.
(19) Edgecombe, K. E.; Weaver, D. F.; Smith, V. H. *Can. J. Chem.* **1994**, *72*, 1388–1403.
(20) Xie, J. R. H.; Smith, V. H.; Allen, R. E. *Chem. Phys.* **2006**, *322*, 254–268.
(21) Morcillo, J.; Gallego, E.; Peral, F. *J. Mol. Struct.* **1987**, *157*, 353–369.
(22) Peral, F.; Gallego, E.; Morcillo, J. *J. Mol. Struct.* **1990**, *219*, 251–256.
(23) Tinoco, I. *J. Am. Chem. Soc.* **1960**, *82*, 4785–4790.
(24) Peral, F.; Gallego, E. *J. Mol. Struct.* **1992**, *274*, 105–114.
(25) Peral, F.; Gallego, E. *J. Mol. Struct.* **1994**, *326*, 59–68.
(26) Peral, F.; Gallego, E. *Biophys. Chem.* **2000**, *85*, 79–92.
(27) Peral, F.; Gallego, E. *Spectrochim. Acta Part A* **2000**, *56*, 747–759.
(28) Branco, L. C.; Afonso, C. A. M. *J. Org. Chem.* **2004**, *69*, 4381–4389.
(29) Maitra, A. *J. Phys. Chem.* **1984**, *88*, 5122–5125.
(30) Stahla, M. L.; Baruah, B.; James, D. M.; Johnson, M. D.; Levinger, N. E.; Crans, D. C. *Langmuir* **2008**, *24*, 6027–6035.
(31) Baruah, B.; Roden, J. M.; Sedgwick, M.; Correa, N. M.; Crans, D. C.; Levinger, N. E. *J. Am. Chem. Soc.* **2006**, *128*, 12758–12765.
(32) Riter, R. E.; Willard, D. M.; Levinger, N. E. *J. Phys. Chem. B* **1998**, *102*, 2705–2714.

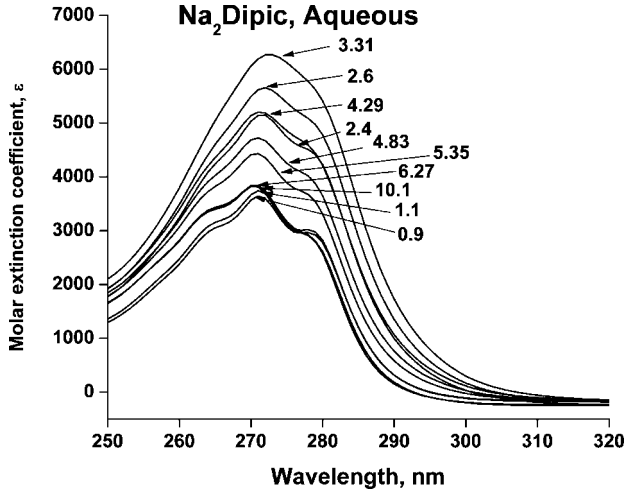

FIGURE 2. Molar extinction coefficient calculated from UV−vis absorption spectra measured in aqueous 0.10 mM dipic at different pH values from 0.9 to 10.1.

dipic both in aqueous solution and in microemulsions using UV−vis and ^{1}H NMR spectroscopy. Through ^{1}H NMR studies, including 1D and 2D NOESY experiments, we directly characterize the interactions between the dipic ligand and AOT molecules in microemulsions. These studies provide data clarifying the structure of dipic isomers in aqueous solution. Importantly, our observations were consistent with the dianionic form of dipic penetrating and residing deep in the AOT lipid interface. These studies confirm previous reports[10−12] that simple aromatic acids are capable of penetrating and existing in hydrophobic environments. This work thus has important consequences for organic reactions and drug penetration.

Experimental Methods

Materials. 2,6-Pyridinedicarboxylic acid (H_2dipic, 99.5% purity) and AOT (sodium bis(2-ethylhexyl)sulfosuccinate, 98% purity) were purchased from a commercial supplier. The AOT was purified as described previously,[30] which includes dissolution of the surfactant in methanol and charcoal, filtration and rotary evaporation until flaky, followed by ^{1}H NMR analysis to check purity. Purified AOT was used for all the reverse micelle investigations and is hereafter referred to as highly purified or HP AOT. Deuterium oxide (D_2O), 2,2,4-trimethylpentane (isooctane), and deuterated 2,2,4-trimethylpentane (isooctane-d_{18}) were also purchased from a commercial supplier and were used as received. Manipulation of aqueous solution pH for NMR samples was performed using dilutions of 35% deuterium chloride in D_2O (99% deuterium) and 30% sodium deuteroxide in D_2O (99% deuterium). Fine-tuning of solution pH for UV−vis analyses used aqueous HCl and/or NaOH before adjusting to the desired final volume.

Preparation of Reverse Micelles (RMs). RMs or microemulsions were prepared as described previously.[30] The 200 and 750 mM stock solutions of HP AOT were prepared by dissolving the surfactant in isooctane. Stock solutions of dipic were prepared by dissolution in water, and pH was adjusted to the desired value. A range of RMs was prepared with w_0 ranging from 6 to 20. Upon mixing these solutions as prescribed, a cloudy solution resulted that cleared after vigorous vortexing. Verification of RM formation was performed using several methods including conductivity measurements[24] (Thermo Orion 150A+ meter with an attached Orion 0111020 cell, range of 10 μs/cm to 200 ms/cm) and viscosity[24] (Cannon−Fenske routine viscometer). These measurements allowed comparison with previous samples of RMs prepared with water to confirm that micelle structure is not appreciably altered by addition of dipic.[30−32]

UV−vis Spectroscopy. Samples for UV−vis spectroscopy were prepared from 200 mM HP AOT stock solution in isooctane at w_0 sizes ranging from 6 to 20 and containing 0.10−0.16 mM dipic in H_2O at the desired pH values. Aqueous dipic stock solutions were prepared in volumetric flasks where pH, and then volumes were adjusted to the desired values. The RMs were prepared just prior to measurements; however, no changes were observed in the samples over the course of 24 h.

UV−vis spectroscopic measurements were carried out using a Perkin-Elmer Lambda 25 UV/vis spectrometer and UV Winlab software. Data was processed using OriginPro (version 7E, Origin Laboratories). Samples were contained in quartz cells with a 1 cm path length. Concentrations of dipic in the samples were generally from 1.5 to 1.0 mM and were adjusted so that the absorbances were less than 1.5 at $\lambda = 271$ nm. Spectra were routinely recorded from 200 to 600 nm. Spectra of all samples were collected in duplicate unless deviations were observed, in which case additional scans were obtained.

^{1}H NMR Spectroscopy. RM samples for NMR spectroscopy were prepared from 750 mM HP AOT stock solutions in isooctane, and 5−25 mM dipic in D_2O at the desired pH values were prepared. The dipic stock solutions were adjusted near the desired pH using DCl and NaOD before the final dilutions were made. The mixtures of AOT in isooctane microemulsion (1 mL volume) were vortexed in sample vials where they were stored before and after ^{1}H NMR spectra were recorded.

^{1}H NMR spectra were recorded on a Varian 400 MHz NMR spectrometer or a Varian Inova-500 MHz spectrometer using the Varian supplied pulse sequence. The 1D spectra were recorded using routine parameters as described previously,[33] and the chemical shift was referenced against an external sample of 3-(trimethylsilyl)propanesulfonic acid (DSS).

^{1}H−^{1}H NOESY NMR experiments were performed on a 400 or 500 MHz Varian Inova NMR spectrometer. The NOESY data were acquired with a 7 kHz window for proton in t_2 and t_1. The NOESY mixing time was varied from 0 to 500 ms. The total recycle time between transients was 2.1 s. The data set consisted of 1000 complex points in t_2 by 256 complex points in t_1 using States-TPPI. Cosine-squared weighting functions were matched to the time domain in both t_1 and t_2, and the time domains were zero-filled prior to the Fourier transform. The final resolution was 3.5 Hz/pt in F2 and 15 Hz/pt in F1. Data processing was done using the Varian VNMRJ-1.1D software, both the Solaris and the Macintosh versions.

Results and Discussion

UV−vis Spectroscopy of Dipic in Aqueous Solution at Varying pH Values. Figure 2 shows the UV−vis spectra of a 0.10 mM aqueous dipic solution adjusted from pH 0.9 to 10.1. Since the concentration of dipic is maintained constant, the spectra illustrate the differences in spectrum shape and extinction coefficients, ε, of dipic as the pH is varied and protonation states and association states changes. A hypsochromic shift in the UV−vis spectra of aqueous solutions of 0.10 mM dipic with pH varying from 0.9 to below 3.3 has previously been attributed to dipic dimerization and was confirmed in Figure 2.[16] Similar results were obtained with nicotinic acid.[24,34,35] Stacking of related pyridine-based systems has been studied in detail and has been observed in dipic and other heteroaromatic rings such as the nucleotide bases in RNA and DNA.[26] At pH values from 1.0 to 2.2 (pK_{a2}), monobasic dipic exists as primarily the zwitterion **2** or the neutral species **5**.[16] Between pH 2.2 and

(33) Crans, D. C.; Yang, L. Q.; Jakusch, T.; Kiss, T. *Inorg. Chem.* **2000**, *39*, 4409–4416.
(34) Green, R. W.; Tong, H. K. *J. Am. Chem. Soc.* **1956**, *78*, 4896–4900.
(35) Stephenson, H. P.; Sponer, H. *J. Am. Chem. Soc.* **1957**, *79*, 2050–2056.

3.3, dipic loses a second proton and may exist as the minus one dipic species **3** or **6**.

The hyperchromic shift observed at pH 3.3 provides clear evidence that dipic exists in the colinear dimeric form shown in structure **7**.[16] Dimerization of the dipic monoanion at pH 3.3−3.5 is supported by the large association constants, $K_a = 2 \pm 1 \times 10^6$, reported at this pH.[16] Our UV−vis results are in agreement with these results and conclusions.

From pH 4.3 to 6.2, ε continues to decrease indicating conversion of the dipic dimer to the fully deprotonated dipic **4**, in agreement with the results reported by Peral and co-workers, who concluded that dipic is undergoing base-stacking interactions in this pH range.[16,23,24,26,36] Polymerization is discounted because no secondary hypochromic effect is observed[23,24] in contrast to that reported for the monocarboxylic picolinic acid (pic). Indeed, pic exists as a monocation below pH 3, as the zwitterion from pH 3 to 7 and as a monoanion above pH 7 and at pHs approaching their isoelectric points, pic and other pyridinecarboxylic acids exist primarily as zwitterions with very low solubility.[24] For several pyridine-related systems, such as dipics,[16−18] the monocarboxylic pyridines picolinic, nicotinic and isonicotinic acids,[24,34,35] and pyridine,[25,37] the aqueous species have been characterized. While UV−vis spectroscopy provides a very sensitive tool for detection of changes in dipic speciation and association, the nature of dipic species are under some debate[16,18,34] and made further characterization of dipic especially compelling. Additional structural information obtained by high-field ^{1}H NMR studies allowed us to distinguish between similarly charged dipic isomeric species and to clarify existing questions regarding dipic structures in both aqueous solutions and reverse micelles.

^{1}H NMR Spectroscopy of Dipic at Varying pH Values in Aqueous Solutions. The ^{1}H NMR spectra of aqueous dipic solutions (at 20 or 25 mM depending on solubility) shown in Figure 3 demonstrate the effect that pH and the varying species has on the chemical shift of the pyridinyl methine proton signals. The observed chemical shift changes are the result of dynamic equilibria between major isomers of a particular charge and protonation state and the association equilibria that occur at a specific pH. In the interpretation of our data we refer to dipic structures **1**−**4** found in Scheme 1, structures **5**−**8** shown in Scheme 2, and structure **9** in Figure 3, which shows the designations H_a, H_b, and H_c for the pyridinyl ring protons. In the interpretation presented here, first the data is interpreted assuming that proton transfer and associative processes are slow and observable on the NMR time scale. However, an asymmetric isomer if undergoing a rapid equilibrium with an opposing asymmetric species will appear symmetric and must be considered.

In Figure 4 we have plotted the chemical shifts of H_a and H_b in aqueous solutions as a function of pH. Because the fully protonated, triprotic dipic species **1** has a pK_a of −1.05,[16] these NMR studies were performed outside of the pH region for this species. In 1D NMR studies of aqueous dipic solutions with pH values from 0.9 to 1.6 we observed an A_2X splitting pattern[38] containing signals for H_b near δ 8.2 ppm and upfield of the H_a protons near δ 8.3 ppm. The pattern is consistent with the symmetrical structure of the neutral dipic, **5**, which contains a

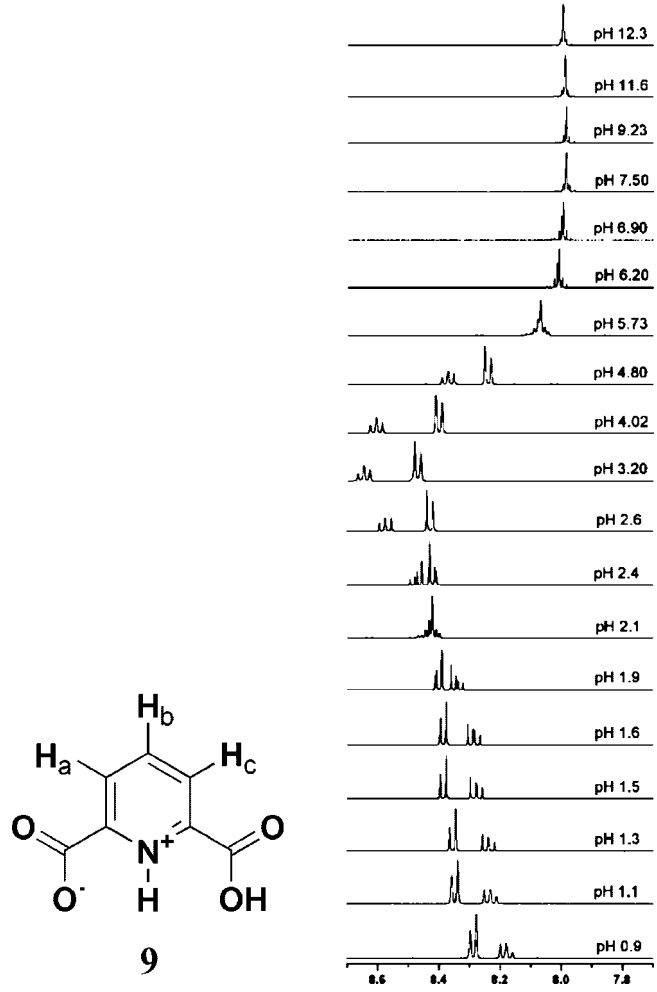

FIGURE 3. 400 MHz ^{1}H NMR spectra recorded in D_2O of 20 mM dipic in aqueous solution at pH values 0.9−2.6, 9.23, and 11.6 and of 25 mM dipic in aqueous solution at pH values 3.20−7.50 and 12.3. Samples were referenced against an external DSS sample. In structure **9**, the three different protons H_a, H_b, and H_c are shown in an amphiphilic form of dipic.

deprotonated pyridine nitrogen. The designations for H_a, H_b, and potentially H_c, when the isomer is asymmetric, are shown in structure **9** in Figure 3 and will vary depending on the protonation and association state of the species. The asymmetrical neutral dipic structure, **2**, containing one protonated carboxyl and a protonated ring nitrogen, contains three different protons H_a, H_b, and H_c and is not consistent with the NMR data observed without invoking dynamic processes. However, a rapid interconversion on the NMR time scale between **2** and **2′** shown in Scheme 3 is consistent with the observed ^{1}H NMR spectra.

As the pH increases above 1.9, the H_b proton signals shift downfield and the first-order spectrum converts into a second-order spectrum with a complex multiplet centered at 8.4 ppm that encompasses the signals for all of the methine protons on the ring. As the pH increases, the downfield shifts in the A_2X pattern resonances indicate that the dipic species is changing from the neutral structure into a minus one species. This conversion to a minus one charged dipic species is consistent with the second reported pK_a for dipic being 2.22. At pH 2.6, the A_2X splitting pattern changes when the H_b signals move further downfield than the H_a signals, Figure 4. At pH 3.20 when the H_b proton is near 8.65 ppm, the species in solution giving

(36) Lindsay, J. A.; Murrell, W. G. *Cur. Micro.* **1986**, *13*, 255–259.
(37) Tokuhiro, T.; Wilson, N. K.; Fraenkel, G. *J. Am. Chem. Soc.* **1968**, *90*, 3622–3628.
(38) *Organic Structure Analysis; 1 ed.*; Crews, P., Rodriguez, J., Jaspars, M. , Ed.; Oxford University Press: New York, 1998.

SCHEME 2. Possible dipic Species at Varying pH Values Structures 5−8

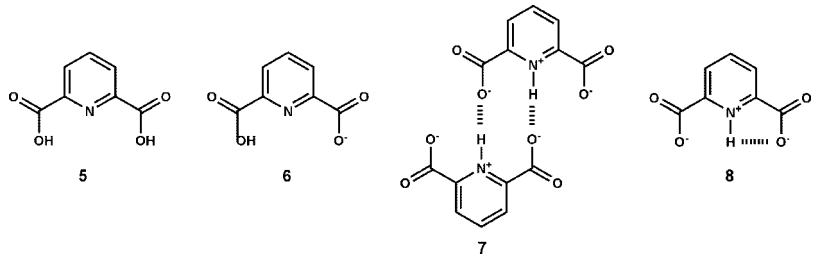

rise to the A_2X system splitting pattern are best described by a symmetric monoanionic structure such as **3**. The asymmetric structure **6** or dimeric structure **7** are not consistent with the NMR data without invoking dynamic processes equilibrating two unsymmetrical species.

At pH values above 5.73, the doublet and triplet merge to form a complex multiplet that encompasses the methine protons in the A_2B system beginning around 7.9 ppm. At pH values above 7.50 the multiplet is centered at δ 8.0 ppm. This multiplet is ascribed to the completely deprotonated dipic species, structure **4**. As pH increases from 5.7 to 7.0, the multiplet simplifies to a broad singlet at pH 7.0 and above. From pH 6.1 to 6.9 a slight downfield shift is observed. However, above pH 7.0 no further chemical shift and signal pattern changes are observed in Figures 3 and 4.

Our ^{1}H NMR studies confirm the changes observed in the absorption spectra of dipic, and provide specific information regarding the structure of the dipic species in solution. Over the entire pH range, the NMR spectra show the presence of an A_2X or A_2B spin system consistent with a symmetric structure or proton symmetry achieved through a rapid equilibration of two asymmetric species. Although the NMR splitting pattern changes dramatically, the spin system remains the same while the chemical shifts of H_a and H_b change.[38] As the pH increases, the chemical shifts of the H_a and H_b protons merge and then separate. In the pH range from 2.6 to 4.8 the chemical shift of H_b is further downfield than the H_a in an A_2X spin system. This pH coincides with the large hyperchromic effect in the UV−vis spectra in Figure 2 and the formation of dimeric species.[16] The dimer structure has an increased electron density at the pyridine N. Hydrogen bonding moves both the H_a and H_b chemical shifts downfield. Since the dimer structure, **7**, is asymmetric, it must undergo equilibration on the time scale of the NMR experiment.

In the literature, the structure for $Hdipic^-$ is generally attributed to the zwitterion shown as structure **2** above. Since this zwitterion is not symmetrical, our results will require that rapid proton transfer reactions convert structure **2** to **2′** as shown in Scheme 3 where H_a and H_c become equivalent as a result of

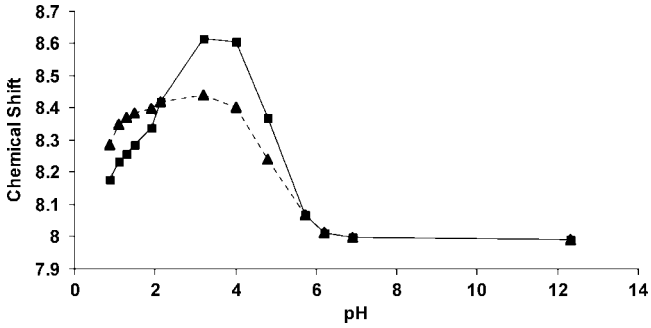

FIGURE 4. Chemical shifts of dipic protons H_a (triangles) and H_b protons (squares) plotted as a function of pH in aqueous solutions.

SCHEME 3. Monoprotonated Zwitterionic Structure of dipic (2) and the Corresponding Structure after Rapid Equilibrium (2′)

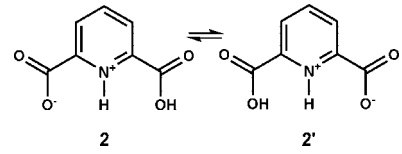

the equilibrium. The NMR data are consistent with both the zwitterionic structure **2** and the diprotonated dicarboxylpyridine shown in structure **5**.

The NMR spectra at high pH values above the third pK_a of dipic reflect the formation of dianionic dipic, **4**. This dianion is symmetrical and, therefore, is consistent with the observed A_2B spin system. The UV−vis spectra in Figure 2 are also consistent with progressive disappearance of the dimer **7** and formation of dianion **4** because the extinction coefficient decreases from the maximum observed at pH 3.2 (3.5 in literature) as pH decreases.[5] At pH's above 6.9, little or no change is seen in both NMR and absorbance spectra indicating that the dianionic species **4** predominates.

In summary, the dipic species observed by NMR studies in aqueous solutions are represented in the Scheme 4 shown below. Although the existence of other monomeric and dimeric species cannot be disregarded, on the basis of our NMR and UV−vis results combined with those reported previously,[17,23,26,27] the species shown in Scheme 4 best explain all the available data.

UV−vis Spectroscopy of Dipic at Varying pH Values in Microemulsions. We have also measured UV−vis absorption spectra of dipic in RMs. For these studies, aqueous dipic stock solutions similar to those shown in Figure 2 were prepared, albeit at a slightly higher concentration because these solutions were to be added to the microemulsions (0.158 mM overall concentration in microemulsion). The spectra recorded, shown in Figure 5, differ from those obtained in aqueous solution, Figure 2. Here, we observe an increase in the extinction coefficients at pH 2.6, a lower value compared to the pH of 3.3 observed in the spectra of aqueous dipic. Furthermore, in the RM suspensions the spectra appear the same for all the samples at pH 4 and above. Several key differences exist between the spectra shown in Figures 2 and 5. First, in the RMs spectral variations occur over a much narrower pH range than in aqueous solutions. Second, the spectra of dipic in the RMs show three distinct maxima λ = 265, 271, and 278 ± 2 nm which are only observed in aqueous solution at very low pH values (<1.1) or at pH's equal to 6.27 and above. Third, the high baseline in the spectrum of the dipic sample at pH 0.8 in RMs indicates that nonhomogeneous RM preparations may form at very acidic pH. The extinction coefficients of sodium dipic (Figure 5) in microemulsions are smaller than those observed in aqueous solution (Figure 2).

SCHEME 4. Dipic Structures and Equilibria in Aqueous Solution with Corresponding pK_a Values

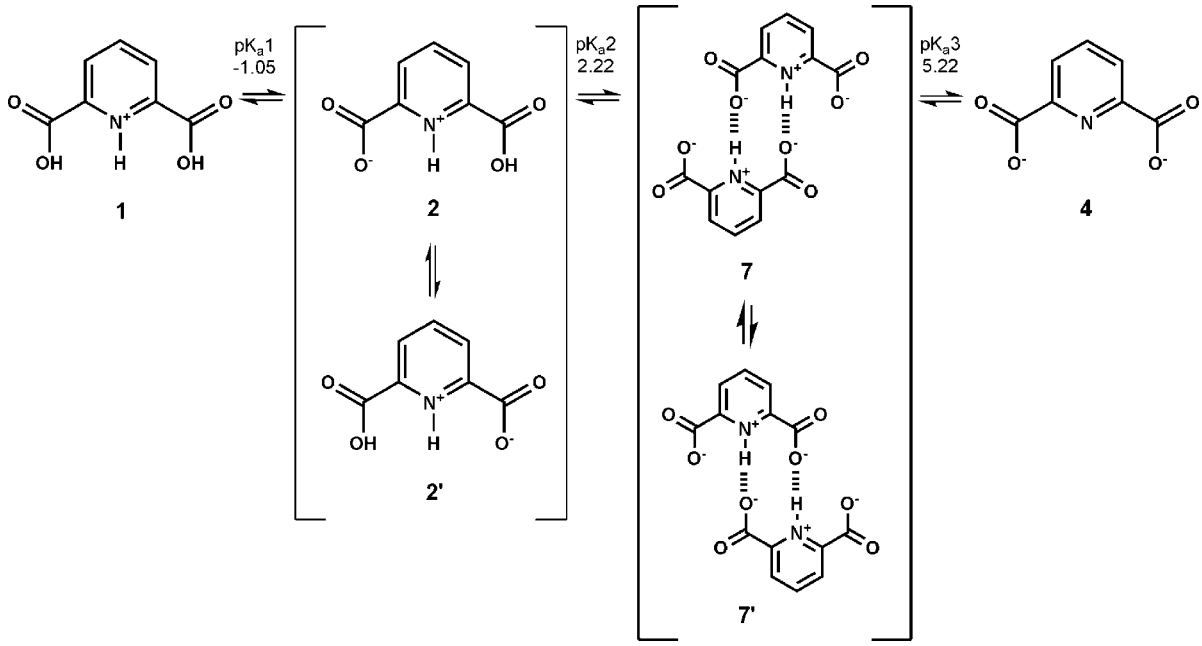

A separate investigation in microemulsions examined the effect of RM size and, therefore, water pool size on the UV−vis absorption by dipic. The absorption spectra were recorded at different w_0 values (6, 12, 16, and 20) for RMs containing 0.10 mM aqueous dipic at pH 2.6 and 3.3. As shown in Figure 6, at each pH value only small changes in the extinction coefficient were observed for RM sizes 12−20. At both pH values, however, we observed a change in the ratio of the peaks as the RM size decreases to $w_0 = 6$. All spectra of dipic in RMs of any size display a hypochromic (also referred to as hypsochromic) shift compared to the spectra in aqueous solutions. Furthermore, the spectrum of dipic in the RMs shows a slightly larger extinction coefficient at pH 2.6 than at pH 3.5.

^{1}H NMR spectra of dipic in 750 mM AOT/isooctane microemulsions were recorded for a series of solutions with pH values ranging from 0.9 to 12.3. The spectra are shown in Figure 7. From pH 0.9 to 1.5, the A_2X splitting pattern was observed with the H_a doublet around 8.4 ppm and the H_b triplet near 8.0 ppm. At pH's from 1.9 to 4.8 a complex splitting pattern was observed until pH 6.9 and higher where a lone singlet at 8.1 ppm was observed. Studies were carried out by NMR spectroscopy at $w_0 = 6$. We anticipated that for small RM sizes if dipic remained in the water pool, some interaction with the interface would be observable since such effects are generally more pronounced at small w_0 sizes.[30] The spectra recorded from dipic in the microemulsions (Figure 7) are very different than those observed for the aqueous samples (Figure 3). The spectra in microemulsions show no severe downfield shifts as observed from pH 3.2 to 4 in aqueous solutions. This observation provides evidence that no dimer species form in the microemulsion. Importantly, the NMR studies of dipic in the microemulsions show that it does not undergo the dimerization processes observed in aqueous solution.

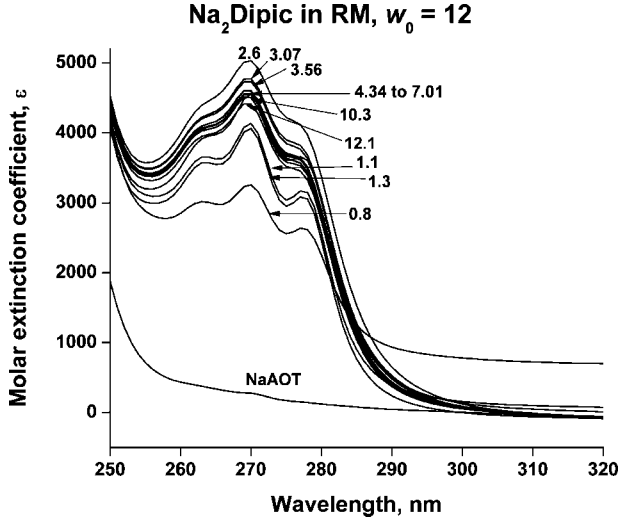

FIGURE 5. Absorption spectra of microemulsions containing 0.158 mM dipic in 200 mM AOT/isooctane. RMs (w_0 =12) were prepared from aqueous stock solutions at pH values from 0.8 to 12.1.

^{1}H NMR spectroscopy of the dipic solutions in the microemulsion show an A_2X or A_2B spin system and are consistent with the UV−vis results for dipic in RMs. Since the concentration of dipic was more than 10-fold higher than those recorded by UV−vis spectroscopy, dimerization would be favored more in the NMR studies than in the UV−vis studies. Under the conditions used for the NMR studies, the average number of dipic molecules per RMs ranged from 0.03 to 0.2 and were thus much below the 2 dipic molecules per RM needed to form a dimer.[29,31,39] Given the low concentration of dipic in the RM, dimerization is not favored under these conditions regardless of the high formation constant in aqueous solution.

2D NOESY Spectroscopy of Dipic Ligand in Microemulsions. In order to investigate whether dipic can penetrate the negatively charged AOT interface, a 2D NOESY experiment was recorded of dipic in AOT/isooctane RMs. The spectrum of aqueous dipic (200 mM) at pH 6.1, in a microemulsion of 1 M AOT with w_0 12, is shown in Figure 8. The 1D spectrum of

(39) Pal, T.; De, S.; Jana, N. R.; Pradhan, N.; Mandal, R.; Pal, A.; Beezer, A. E.; Mitchell, J. C. *Langmuir* **1998**, *14*, 4724–4730.

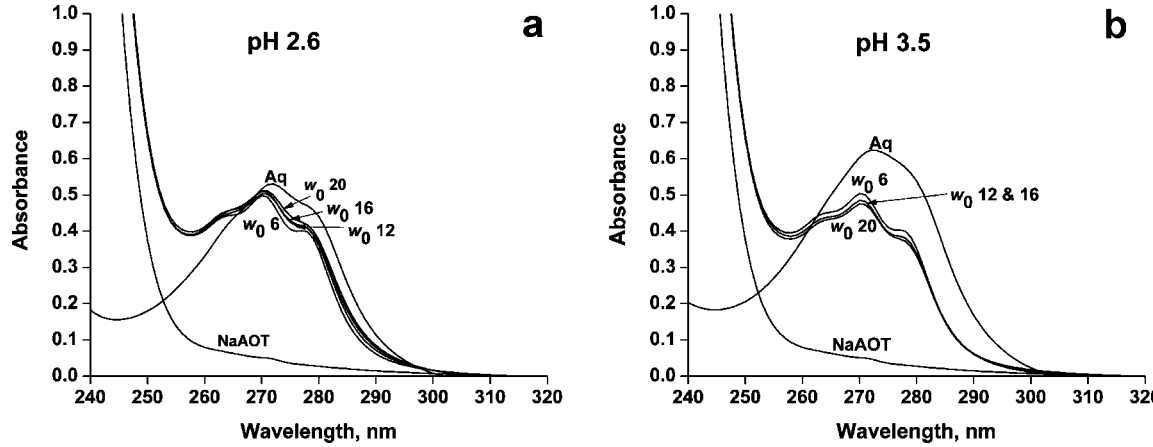

FIGURE 6. Absorption spectra of 0.10 mM dipic in 200 mM AOT/isooctane RMs. Aqueous dipic solutions at pH (a) 2.6 and (b) 3.5 were used to prepare microemulsions with $w_0 = 6$, 12, 16, and 20.

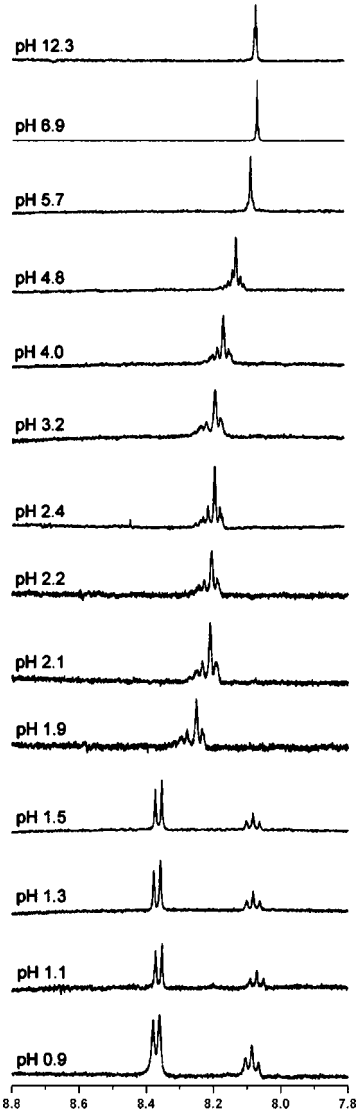

FIGURE 7. 400 MHz ^{1}H NMR spectra of dipic in 750 mM AOT/isooctane microemulsions with $w_0 = 6$. Aqueous stock solutions of 20−25 mM dipic from pH 0.9 to 12.3 were used to prepare RMs with final dipic concentrations of 1.45−1.81 mM. Samples at pH 3.20−6.20 were prepared with the higher concentration stock solution; the rest were prepared with 20 mM dipic. Samples were referenced using isooctane.

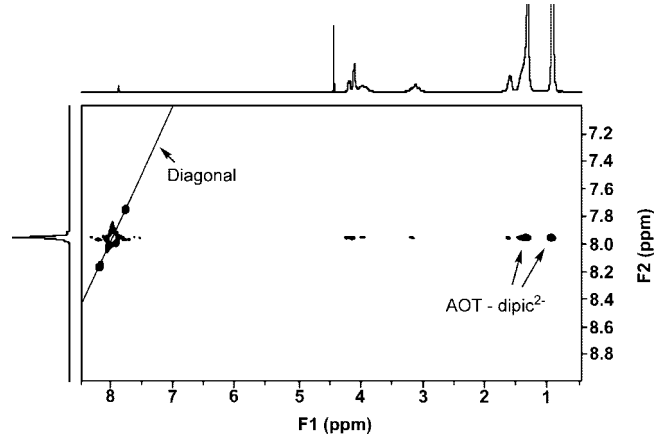

FIGURE 8. Section of the 2D NOESY of 200 mM dipic in 1 M AOT/isooctane-d_{18} in D_2O/pH 6.1. $w_0 = 12$ adjusted to pH 6.1 with NaOD.

this solution results in only one signal at about 8.2 ppm that is consistent with fully deprotonated dipic with a minus two charge.

The 2D NOESY spectrum includes many cross signals arising from interactions between protons on AOT. To examine whether dipic can penetrate the AOT interface and traverse up into the hydrophobic chains of AOT, for simplicity, we show the portion of the 2D NOESY spectrum (Figure 8) containing the signal for the dianionic dipic around 8.2 ppm and on the opposing axis, the entire chemical shift range for AOT. In addition to the main signal at 8.2 ppm, we observe two small peaks attributed to ^{13}C satellite signals for dipic. In the 2D spectrum, the major cross peaks to the dipic signal corresponded to signals for the methylene and methyl groups in the AOT. These signals indicate that the deprotonated dipic successfully penetrates the negatively charged AOT interface and resides deep in the AOT interface. Some additional minor cross signals are observed in Figure 8 with the other parts of the AOT molecule and provide support for the hypothesis that the dianionic dipic does indeed travel up into the surfactant interface.

The aqueous dipic solutions used for this study were at 200 mM, and AOT was at 1 M with a $w_0 = 12$ in order to provide the sensitivity required for the 2D experiment. Our aqueous UV−vis studies suggested that dimerization should be a significant factor at this concentration. However, interactions of dipic with AOT may compete with hydrogen bonding

between dipic molecules, thus making dimerization less likely. As observed in Figure 8, cross peaks between the dipic and AOT methyls and methylenes were observed. This result confirms that dipic resides deeply within the AOT interface and thus can penetrate the negatively charged AOT surface. Since it would be advantageous for dipic to protonate before penetration of the AOT layer, we examined the chemical shift of the dipic species that interacted with the AOT CH_2 and CH_3 groups. Because only one dipic signal was observed at a $\delta = 8.2$ ppm, this is indeed consistent with the doubly deprotonated dipic species, structure **4**, residing deep into the AOT interface layer.

Attempts were made to prepare microemulsions as above using dipic solutions with a range of pH values. Microemulsions with high (200 mM) concentrations of dipic could only be successfully prepared at pH values above the second pK_a where the double-deprotonated dipic species predominates.

In the literature, several approaches have been used to examine Overton's rule and the ability of simple aromatic acids to penetrate membranes and lipid interfaces.[10−12] Classical electrostatic principles and some studies strongly favor protonation of these acids prior to penetration of the lipid interface and localization in a hydrophobic environment. The structural results obtained in our studies are unexpected. Our results suggest that not only dipic, but dipic in the dianionic form, is able to penetrate the surface. Why would a minus two charged molecule penetrate a negatively charged interface and reside in a hydrophobic environment deep inside the lipid layer? We propose the following explanations. The RMs are very dynamic structures that undergo forming and reforming processes on a millisecond time scale. It is possible that such events would allow dipic to associate sufficiently strongly with the AOT for penetration to take place. Alternatively, dipic could associate with cations and thus exist as an ion pair capable of lipid interface penetration. Evidence for such events has been reported[40,41] and ion pairs are commonly proposed in organic chemistry to explain effects in transition states or high energy intermediates. These considerations are important and will be investigated for our dipic system in the future. Our data suggest that the location of the highly charged dipic species is deep within the AOT interface. This finding goes against the existing dogma and contributes information regarding the unusual behavior of organic acids at lipid interfaces. Since $[VO_2dipic]^-$ has previously been found to penetrate the lipid interface and the free $dipic^{2-}$ ligand has been observed in those experiments,[2] our current finding shows that the vanadium is not necessary for penetration.

Studies with the dipic ligand are important to be able to elucidate what part of biological activity is due to the metal complex or the ligand. The dipic system is particularly suitable to probe the question of interface penetration, because the dipic ligand NMR spectrum is particularly sensitive to protonation state and, thus, provides information as to (1) what ion species is present, (2) whether it penetrates the reverse micelle hydrophobic interface, and (3) its potential to penetrate lipid bilayers in biological systems.

Hydrogen bonding has been invoked in the specific structures that form in bacteria where dipic is part of the spore.[36,42,43] Undoubtedly, dipic's ability to associate and form isomers[5] in the presence and absence of Ca^{2+} plays an important role in spore development. In the studies presented here, the finding that dianionic dipic is capable of penetrating the lipid interface goes beyond potential applications of the metal complexes as therapeutic agents. Previous studies with both mono- and dicarboxylic acids all point to membrane transport of only the neutral form.[10−12,31,40,41,44] However, our studies provide structural data that unequivocally show that dipic is in the dianionic form when associated with the hydrophobic part of AOT in location C depicted in Figure 1b. Our studies document that this simple charged aromatic carboxylate is stabilized sufficiently to exist in the hydrophobic environments. This work therefore provides an important contribution to the current debate examining the violations of the Overton and the Lipinski rules.

Conclusion

As shown in Scheme 1, these studies reevaluated the speciation of dipic from acidic pH to basic pH in aqueous solution. The structural information obtained by NMR spectroscopy shows that the species in solution is a symmetric species attainable by rapid equilibration of two asymmetric isomers. A summary of these results are shown in Scheme 4.

Upon addition of these solutions to the microemulsions, the resulting NMR spectra resembled those in aqueous solution except for the pH region from 2.6 to 6. In this region, the spectra of ligand in microemulsions are very different from the aqueous dipic solutions. In addition, a 2D NOESY experiment was recorded and showed that the dipic molecules reside deep inside the lipid interface. Importantly, the penetrating form of dipic, as evidenced by the NMR chemical shifts, is the fully deprotonated H_2Dipic with a minus 2 charge. Thus, these results provide data that show a double negatively charged aromatic acid is capable of penetrating a lipid interface. Although we did not attempt to study the mechanism of the penetration, the fact remains that this polar and charged aromatic carboxylate is sufficiently stabilized in a very hydrophobic environment to overcome other seemingly attractive options. Future studies will explore the potential ion pairing of the acid and will determine the effects of electronic charges in the solubility of this multifaceted, dynamic molecule.

Lastly, characterization of dipic behavior in mixed phase systems, such as microemulsions, is of special relevance to organic chemistry especially in reactions where heterogeneous catalysis or less conventional conditions are employed. Therefore, microemulsions serve as valuable model systems where solubility assumptions may be tested for charged organic molecules.

Acknowledgment. This material is based upon work supported by the National Science Foundation under Grant No. 0628260. We thank Christopher R. Roberts for technical assistance and reading this manuscript.

JO801707Y

(40) Yang, X. G.; Wang, K.; Lu, J. F.; Crans, D. C. *Coord. Chem. Rev.* **2003**, *237*, 103–111.
(41) Yang, X. G.; Yang, X. D.; Yuan, L.; Wang, K.; Crans, D. C. *Pharm. Res.* **2004**, *21*, 1026–1033.
(42) Murrell, W. G. In *The Bacterial Spore*; Gould, G. W. H., A., Ed.; Academic Press, Inc.: New York, 1969; pp 215−273.
(43) Hanson, R. S.; Halvorso, Ho; Curry, M. V.; Garner, J. V. *Can. J. Microbiol.* **1972**, *18*, 1139–1143.
(44) Evtodienko, V. Y.; Bondarenko, D. I.; Antonenko, Y. N. *Biochim. Biophys. Acta* **1999**, *1420*, 95–103.